Role for AMP-activated protein kinase in glucose-stimulated insulin secretion and preproinsulin gene expression

Gabriela DA SILVA XAVIER, Isabelle LECLERC, Aniko VARADI, Takashi TSUBOI, S. Kelly MOULE and Guy A. RUTTER[1]

Henry Wellcome Laboratories of Integrated Cell Signalling and Department of Biochemistry, University Walk, University of Bristol, Bristol BS8 1TD, U.K.

AMP-activated protein kinase (AMPK) has recently been implicated in the control of preproinsulin gene expression in pancreatic islet β-cells [da Silva Xavier, Leclerc, Salt, Doiron, Hardie, Kahn and Rutter (2000) Proc. Natl. Acad. Sci. U.S.A. **97**, 4023–4028]. Using pharmacological and molecular strategies to regulate AMPK activity in rat islets and clonal MIN6 β-cells, we show here that the effects of AMPK are exerted largely upstream of insulin release. Thus forced increases in AMPK activity achieved pharmacologically with 5-amino-4-imidazolecarboxamide riboside (AICAR), or by adenoviral overexpression of a truncated, constitutively active form of the enzyme (AMPKα1.T^{172}D), blocked glucose-stimulated insulin secretion. In MIN6 cells, activation of AMPK suppressed glucose metabolism, as assessed by changes in total, cytosolic or mitochondrial [ATP] and NAD(P)H, and reduced increases in intracellular [Ca^{2+}] caused by either glucose or tolbutamide. By contrast, inactivation of AMPK by expression of a dominant-negative form of the enzyme mutated in the catalytic site (AMPKα1.D^{157}A) did not affect glucose-stimulated increases in [ATP], NAD(P)H or intracellular [Ca^{2+}], but led to the unregulated release of insulin. These results indicate that inhibition of AMPK by glucose is essential for the activation of insulin secretion by the sugar, and may contribute to the transcriptional stimulation of the preproinsulin gene. Modulation of AMPK activity in the β-cell may thus represent a novel therapeutic strategy for the treatment of type 2 diabetes mellitus.

Key words: AMP, glucose, insulin, islet, kinase, secretion.

INTRODUCTION

Pancreatic islet β-cells respond to high glucose concentrations by secreting insulin [1] and increasing the expression of preproinsulin (PPI) and other genes [2,3]. Stimulation of insulin secretion by glucose involves the enhanced synthesis of ATP by mitochondria [4] and closure of ATP-sensitive K^+ channels (K_{ATP}) [5]. Subsequent depolarization of the plasma membrane [6] then opens voltage-sensitive (L-type) Ca^{2+} channels [7] causing insulin-containing vesicles to fuse at the plasma membrane [1].

The mechanisms that link changes in glucose concentration to the regulation of β-cell genes are less well understood [8,9]. Recently, we have demonstrated that AMP-activated protein kinase (AMPK) is involved in the regulation of gene expression by glucose in this cell type [10]. AMPK is a multisubstrate, heterotrimeric serine/threonine protein kinase, consisting of a catalytic α-subunit and non-catalytic β- and γ-subunits [11,12]. Enzyme activity is regulated both allosterically by AMP, and through reversible phosphorylation at Thr-172 of the α subunit by an upstream kinase (AMPK kinase, or AMPKK) [13–15]. Active AMPK phosphorylates and inactivates a number of metabolic enzymes involved in cholesterol and fatty acid synthesis, including 3-hydroxy-3-methylglutaryl-coenzyme A (HMG-CoA) reductase [16], and acetyl-CoA carboxylase (ACC) [17,18], thus reducing cellular ATP consumption [18,19] during conditions of metabolic stress [20,21].

Suggesting a potential role in the regulation of insulin release, AMPK activity is inhibited by elevated glucose concentrations in clonal MIN6 [10], INS-1 and HIT-T15 β-cell lines [22]. Moreover, two reports [22,23] have suggested that increases in AMPK activity, achieved using the pharmacological activator 5-amino-4-imidazolecarboxamide riboside (AICAR), may lead to the acute inhibition of insulin secretion. However, two earlier reports [24,25] suggested that AICAR may, rather, potentiate glucose-stimulated insulin secretion from isolated rat islets or perfused pancreata.

Here, we examine the effects of forced changes in AMPK activity through molecular means, via the transduction of MIN6 β-cells or islets with active or inactive forms of the enzyme [26]. Our results suggest that active AMPK acts as a pleiotropic repressor of insulin release and insulin gene expression at low glucose concentrations, whose actions are gradually decreased as glucose concentrations rise.

MATERIALS AND METHODS

Materials

Dulbecco's modified Eagle's medium (DMEM) was from Sigma (Poole, Dorset, U.K.) or Invitrogen (Paisley, U.K.). LIPOFECTAMINE 2000™ was from Invitrogen, beetle luciferin was from Promega (Southampton, U.K.) and coelenterazine was from Molecular Probes (Eugene, OR, U.S.A.). AICAR was supplied by Sigma or Toronto Research Chemicals (Ontario, Canada) and LY294002 by Calbiochem (La Jolla, CA, U.S.A.). Sheep anti-phospho-Thr-172 antibody [27] was generously provided by Professor D. G. Hardie (University of Dundee, Dundee, U.K.). Polyclonal pan-anti-AMPKα antibodies were from Upstate Biotechnologies (Milton Keynes, U.K.) and AMPKβ antibodies were kindly provided by Dr D. Carling (Imperial College, London, U.K.). Alexa Fluor 568 goat anti-rabbit IgG was from Molecular Probes. Collagenase (from *Clostridium histolyticum*; EC 3.4.24.3) was from Serva (Heidelberg, Germany), and other reagents were from Sigma or BDH (Poole, Dorset, U.K.).

Abbreviations used: ACC, acetyl-CoA carboxylase; AICAR, 5-amino-4-imidazolecarboxamide riboside; AMPK, AMP-activated protein kinase; AMPK CA, constitutively active AMPK; AMPK DN, dominant-negative AMPK; $[Ca^{2+}]_c$, cytosolic free Ca^{2+} concentration; DMEM, Dulbecco's modified Eagle's medium; eGFP, enhanced green fluorescent protein; hGH, human growth hormone; K_{ATP}, ATP-sensitive K^+ channel; KRB, Krebs–Ringer bicarbonate; PPI, preproinsulin.

[1] To whom correspondence should be addressed (e-mail g.a.rutter@bris.ac.uk).

© 2003 Biochemical Society

Plasmids

Plasmid pcDNA3.hGH [28] was a gift from Professor R. D. Burgoyne, University of Liverpool, Liverpool, U.K. Plasmids encoding c-Myc-tagged forms of dominant-negative-acting AMPKα1 (AMPK DN) with an Asp-157-to-Ala mutation ($D^{157}A$; pcDNA3.AMPK DN) [26] and truncated, constitutively active AMPK$\alpha 1^{312}$ (residues 1–312; AMPK CA) with a Thr-172-to-Asp mutation ($T^{172}D$; pcDNA3.AMPK CA) [29] were kind gifts from Dr D. Carling, Imperial College School of Medicine, University of London, London, U.K. Plasmid pINS-Luc_{FF} contained nucleotides -260 to $+60$ of the human insulin promoter fused upstream of a minimal herpes simplex thymidine kinase promoter and humanized firefly luciferase cDNA [30]. The expression plasmid for *Renilla reniformis* luciferase (pRL.CMV) was from Promega.

Construction of adenoviruses

pcDNA3.AMPK DN and pcDNA3.AMPK CA were digested with *Kpn*I and *Not*I. Released fragments were subcloned into pShuttle-CMV [31] from which corresponding adenoviruses were generated by homologous recombination in *Escherichia coli* using the pAd.Easy system (http://www.coloncancer.org), and amplification in HEK-293 cells [31,32]. To generate viruses and plasmids encoding enhanced green fluorescent protein (eGFP) in addition to AMPK mutants, *Kpn*I–*Xho*I fragments from pcDNA3.AMPK CA and pcDNA3.AMPK DN were subcloned into the shuttle vector pAd.Track.CMV [31] prior to recombination. Virus particles were purified by CsCl density gradient, and viral particles quantified by titration in HEK-293 cells for eGFP-bearing viruses, or comparison of A_{260} values with viral stocks of known concentration (viruses not bearing eGFP).

MIN6 cell culture and islet isolation

MIN6 β-cells [33] were used between passages 19 and 30 and grown in DMEM containing 15% (v/v) heat-inactivated foetal calf serum (Life Technologies, Paisley, U.K.), 25 mM glucose, 5.4 mM KCl, 2 mM glutamine, 50 μM β-mercaptoethanol, 100 i.u. $\cdot$ ml^{-1} penicillin and 100 μg $\cdot$ ml^{-1} streptomycin. Cells were cultured in a humidified atmosphere at 37 °C with 5% CO_2.

Pancreatic islets of Langerhans were isolated from male Wistar rats (200–230 g) by perfusion of the pancreatic duct and *in situ* collagenase digestion [34]. Islets were subsequently purified by two Histopaque (Sigma) density gradients and hand picking, as described in [35]. Immediately after isolation, islets were cultured overnight in DMEM supplemented with 30% (v/v) heat-inactivated foetal calf serum, 100 i.u. $\cdot$ ml^{-1} penicillin, 100 μg $\cdot$ ml^{-1} streptomycin and 11 mM glucose.

Adenoviral infection

Cells or islets were incubated with adenoviruses at a multiplicity of infection of 30–100 viral particles/cell for 16 h prior to culture for a further 24 h in the absence of added virus, in DMEM containing 3 mM glucose.

Assay of insulin and human growth hormone (hGH) secretion

MIN6 cells, seeded in 12-well microtitre plates, were grown to 50–70% confluency and co-transfected with 1.0 μg of pcDNA3.hGH and either 1.0 μg of pcDNA3.AMPK CA or pcDNA3.AMPK DN, using LIPOFECTAMINE 2000™ according to the manufacturer's instructions. Culture was continued for 24 h in DMEM containing 25 mM glucose, and then at 3 mM glucose for a further 16 h. Cells were then washed in PBS and incubated in modified Krebs–Ringer bicarbonate (KRB) medium comprising 132.5 mM NaCl, 3.6 mM KCl, 0.5 mM NaH_2PO_4, 0.5 mM $MgSO_4$, 1.5 mM $CaCl_2$, 10 mM Hepes and 2 mM $NaHCO_3$, pre-equilibrated with 95%:5% O_2/CO_2, pH 7.4, and either 3 or 30 mM glucose. Incubations were performed for 20 min at 37 °C in a shaking water bath. hGH released into the incubation medium was assayed using a hGH ELISA kit (Roche Diagnostics, Lewes, E. Sussex, U.K.) [28].

Secreted and total insulin were measured by radioimmunoassay, as described previously [32].

Western (immuno-) blotting and AMPK assay

Cells were washed twice in ice-cold PBS, scraped into ice-cold lysis buffer [10], vortex-mixed and centrifuged (14000 ***g***; 3 min; 4 °C). Protein content was assayed using a BCA™ protein assay kit (Pierce, Rockford, IL, U.S.A.), against BSA Type V (Sigma) standards. Total protein extracts (20 μg) were resolved by SDS/PAGE (10%, v/v, bisacrylamide/acrylamide, 37.5:1) and transferred to PVDF membranes [36], followed by immunoblotting [37]. Secondary antibodies were revealed using BM Chemiluminescence blotting substrate (Roche Diagnostics). Total AMPK activity was assayed in crude cell extracts (5 μg of protein) by SAMS peptide assay, using synthetic peptide HMRSAMSGLHLVKRR [10].

Immunocytochemistry

Cells were fixed with formaldehyde and permeabilized with Triton X-100 as described in detail elsewhere [38], before imaging on a Leica TCS-NT laser-scanning confocal microscope using a $\times 63$ PL-Apo 1.4 numerical aperture oil-immersion objective.

Assay of malonyl-CoA

Fatty acid synthase was purified from epididymal fat pads of 200–250 g Wistar rats. In brief, isolated tissue was suspended in extraction buffer (50 mM Mops, 250 mM glycerol, 2 mM EDTA and 1 mM dithiothreitol, pH 7.4) and sheared with a Polytron (Polytron Aggregate Kinematica). Fatty acid synthase was precipitated by $(NH_4)_2SO_4$ precipitation (30–50% saturation) and centrifugation at 18000 ***g*** (10 min). The precipitate was solubilized in extraction buffer and dialysed overnight at 4 °C, before fractionation by cation-exchange chromatography (Mono Q™). Fractions containing fatty acid synthase activity, as determined spectrophotometrically (ΔA_{340} for the following reaction: malonyl-CoA + acetyl-CoA + 2NADPH + $H^+ \rightarrow$ 4-carbon-CoA + CO_2 + $NADP^+$) were kept at -80 °C. Prior to assay, cells were disrupted by repeated freeze–thawing cycles in luciferase assay buffer (100 mM KH_2PO_4, pH 6.8, 715 nM β-mercaptoethanol, 23 μM dodecyl aldehyde and 2 μM FMN). Protein was measured at 560 nm using BSA as a standard. Assays were performed with 300 μg of protein, in a total volume of 2.0 ml, using *Vibrio fischeri* luciferase-NAD(P)H and scintillation counting (Beckman-Coulter LS 6500; Fullerton, NJ, U.S.A.) according to Hughes [39].

Single-cell promoter analysis

Intranuclear microinjection was performed using an Eppendorf 5121/5246 micromanipulator [40]. Plasmids were dissolved at the concentrations indicated in 2 mM Tris/HCl, pH 8.0/0.2 mM

© 2003 Biochemical Society

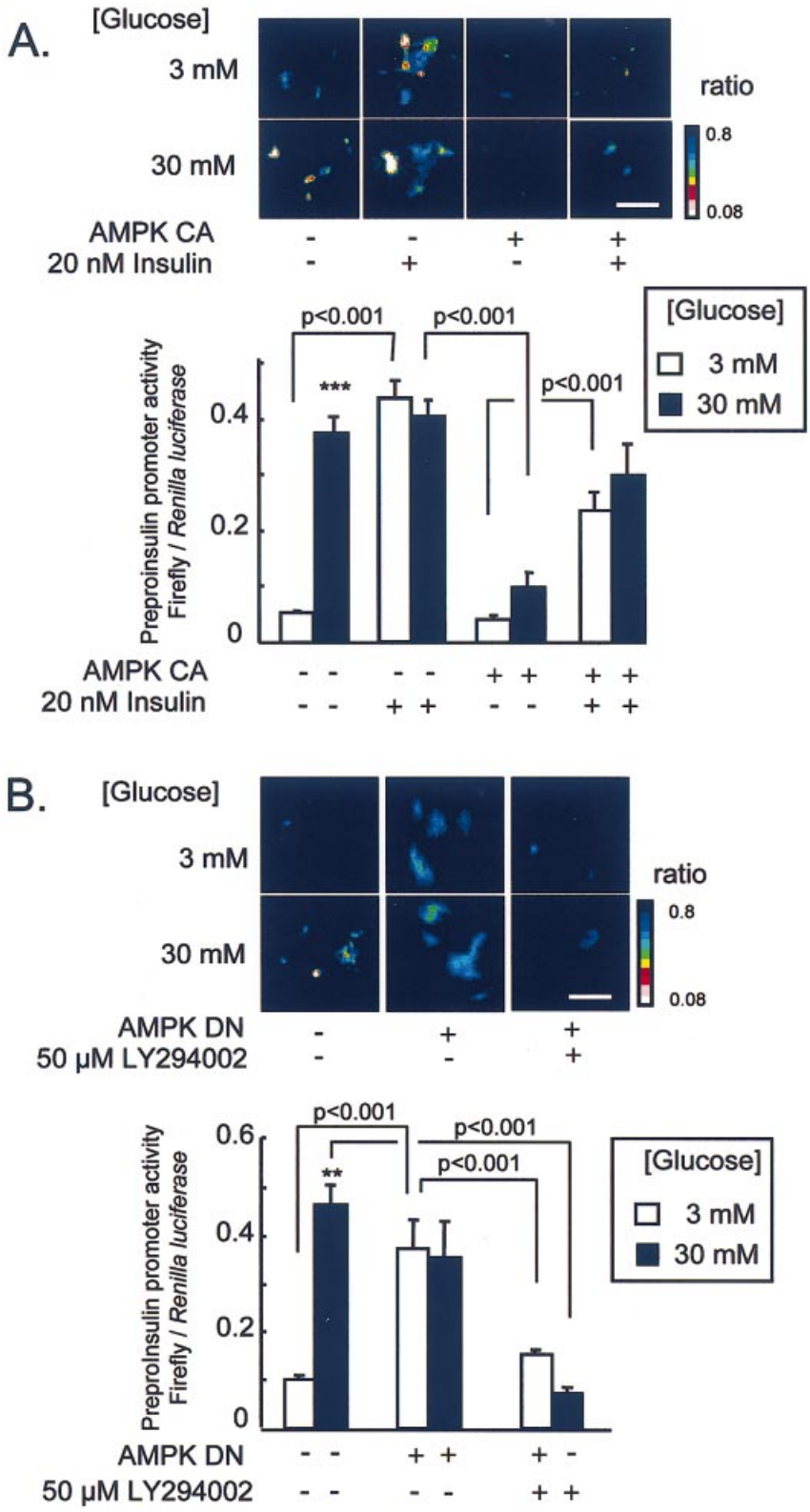

Figure 1 Effect of AMPK CA, AMPK DN and insulin on glucose-regulated PPI promoter activity

Single MIN6 cells were co-microinjected with plasmids pINS.Luc$_{FF}$ (100 μg · ml^{-1}) and pRL.CMV (10 μg · ml^{-1}) plus either empty vector or the indicated AMPK expression vector (100 μg · ml^{-1} each; see the Materials and methods section). After 6 h culture under the conditions indicated, firefly luciferase activity and total (firefly + *R. reniformis* luciferase) activities were quantified sequentially by digital luminescence imaging (see the Materials and methods section) for 200 s in the presence of firstly 1 mM luciferin, then luciferin plus 5 μM coelenterazine [34]. Normalized PPI promoter activity (images) was calculated off-line from the mean ratio of firefly/*R. reniformis* activity in each cell. Data are means ± S.E.M. from three separate experiments in each case, involving a total of 20–100 individual cells. $^{**}P < 0.01$ and $^{***}P < 0.001$ for the effect of 30 versus 3 mM glucose. Scale bars, 100 μm.

© 2003 Biochemical Society

sodium EDTA. Then, 6 h after microinjection and culture under the conditions given, photon-counting imaging of firefly and *R. reniformis* luciferase activities was performed in single living cells using an Olympus IX-70 inverted microscope ($\times 10$ air objective, 0.4 numerical aperture) and an intensified charge-coupled device camera (Photek ICCD316; Photek, Lewes, E. Sussex, U.K.) as described previously [40,41]. Individual experiments involved injection of 100–200 separate cells per condition, with an efficiency of 10–30 % productive injection.

Measurement of cytosolic [Ca^{2+}] ([Ca^{2+}]$_c$), cytosolic and mitochondrial free [ATP], total ATP and mitochondrial NAD(P)H

Changes in [Ca^{2+}]$_c$ were measured after co-microinjection of interfering constructs with a plasmid encoding eGFP (pEGFP.N1; Clontech) to permit identification of microinjected cells. Cells were loaded with fura-2 as described in [32] and imaged at 37 °C in modified KRB medium (see above) using a TILL Photonics imaging system, based on an Olympus IX-70 inverted optics microscope ($\times 40$ oil-immersion objective; Olympus UK, U-APO/340, numerical aperture = 1.35; 490 nm dichroic mirror). A monochromator (Polychrome IV; TILL Photonics, Munich, Germany) was used to provide excitation alternately (0.2 frame $\cdot$ s^{-1}) at 340 and 380 nm. Emission at > 515 nm was detected with an Imago SensiCam KL320 charge-coupled device camera. Autofluorescence due to NAD(P)H was measured using the same system, but in this case 360 nm light was used for excitation, and emission at 450 nm was measured and analysed using TillPhotonic software.

Changes in cytosolic [ATP] or intramitochondrial [ATP] were measured after co-microinjection of plasmids expressing humanized firefly luciferase (Promega) under cytomegalovirus promoter control and bearing either no additional targeting information (pCMV.Luc$_{FF}$) or the mitochondrial targeting sequence of cytochrome c oxidase subunit VIII (pCMV.mitoLuc$_{FF}$) [4]. Single-cell photon-counting imaging was performed using an Olympus IX-70 microscope fitted with a $\times 20$ objective and Photek ICCD218™ intensified camera [40].

For total ATP assay, MIN6 cells were infected with adenoviruses and incubated at the glucose concentrations before extraction into perchloric acid (10 %, v/v). ATP was quantitated in extracts (10 μg of protein) neutralized with Hepes-buffered KOH, using partially purified firefly luciferase (Promega) and photon counting, as described in [42].

Statistical analysis

Data are given as means $\pm$ S.E.M. from at least three individual experiments. Comparisons between means were performed using one-tailed Student's *t* test for paired data with Microsoft Excel™ software.

RESULTS

Regulation of prepropinsulin gene expression by glucose, insulin and AMPK

As previously reported, either elevated glucose concentrations [30,43] or exogenously added insulin [43] caused marked increases in the transcriptional activity of the PPI promoter assayed in single MIN6 cells using luciferase reporter constructs (Figure 1). Co-microinjection of a plasmid expressing a constitutively active form of AMPKα1 (AMPK CA), encoding amino acids 1–312 and bearing an activating mutation ($T^{172}D$) at the regulatory Thr residue [26], led to a near-total suppression of glucose-stimulated PPI promoter activity (Figure 1A), but only partly reversed the effects of added insulin (Figure 1A).

In contrast, microinjection of a plasmid encoding a dominant-negative form of AMPKα1 (AMPK DN), bearing an Asp-to-Ala mutation at the active site ($D^{157}A$) [26], caused a marked activation of the PPI promoter at low glucose concentrations (Figure 1B), an effect similar to that of the microinjection of AMPK antibodies [10]. The effects of both AMPK DN and elevated glucose concentrations were fully reversed by a selective inhibitor of type I phosphoinositide 3′-kinase activity, LY294002 [44], consistent with AMPK DN acting to promote the release of insulin and consequent signalling via insulin (or insulin-like growth factor-1) receptors to phosphoinositide 3′-kinase.

AMPK phosphorylation is regulated by glucose but not by insulin

The above data are compatible with: (i) the regulation of the PPI gene by glucose through a mechanism involving the activation of insulin release, and the subsequent stimulation of a signalling cascade by β-cell insulin receptors [43,45,46] or (ii) the regulation of AMPK by released insulin and consequent effects on PPI gene transcription.

Whereas the latter possibility seemed the less likely, given that the principal regulatory phosphorylation site (Thr-172) of AMPK is mutated in AMPK CA, it was tested formally by monitoring the contribution of insulin release to the regulation of AMPK by glucose (Figure 2). Extracts of MIN6 cells previously incubated at increasing glucose concentrations were immunoblotted with an antibody specific for the phosphorylated form of AMPKα (PT-172). Consistent with our earlier demonstration of glucose-induced inhibition of both AMPKα isoforms in MIN6 cells (α1 and α2) [10], incubation at elevated glucose concentrations (30 versus 3 mM glucose) caused a significant decrease in AMPK activity which was mimicked by adenovirus-mediated expression of AMPK DN, but reversed by AICAR (Figure 2A). Correspondingly, increasing glucose concentrations over the physiological concentration range caused a progressive decrease in the extent of AMPK phosphorylation on Thr-172, most markedly between 5 and 15 mM glucose (Figure 2B). This effect of glucose could not be ascribed to the release of insulin, since addition of increasing concentrations of the hormone failed to decrease the phosphorylation of AMPK at Thr-172 in cells incubated at 3 mM glucose (Figure 2C). Moreover, complete suppression of glucose-induced insulin secretion with the K_{ATP} channel opener diazoxide had no impact on the ability of elevated glucose concentrations to cause dephosphorylation of AMPK (Figure 2D). Together, these data indicate that the inhibition of AMPK by elevated glucose concentrations may result largely from an activation of intracellular metabolism, involving an increase in ATP synthesis [4,47,48] and a corresponding decrease in intracellular AMP levels [22].

Effects of AICAR and active and inactive AMPK, expressed via adenoviruses, on glucose-induced insulin secretion

The findings presented above suggested that the effects of changes in AMPK activity on PPI gene expression are, at least in part, due to alterations in the rate of insulin release, and consequently signalling by β-cell insulin receptors [45,46]. To examine the acute effects of activating AMPK on insulin secretion, we first used the pharmacological activator, AICAR, which is taken up by cells and phosphorylated to the AMP analogue, ZMP (AICAR monophosphate) [13]. Addition of increasing concentrations of AICAR to cells maintained for 1 h at 30 mM glucose caused a progressive elevation in the phosphorylation of AMPK on Thr-172 (Figure 3A) to levels similar to those seen at 3 mM glucose.

© 2003 Biochemical Society

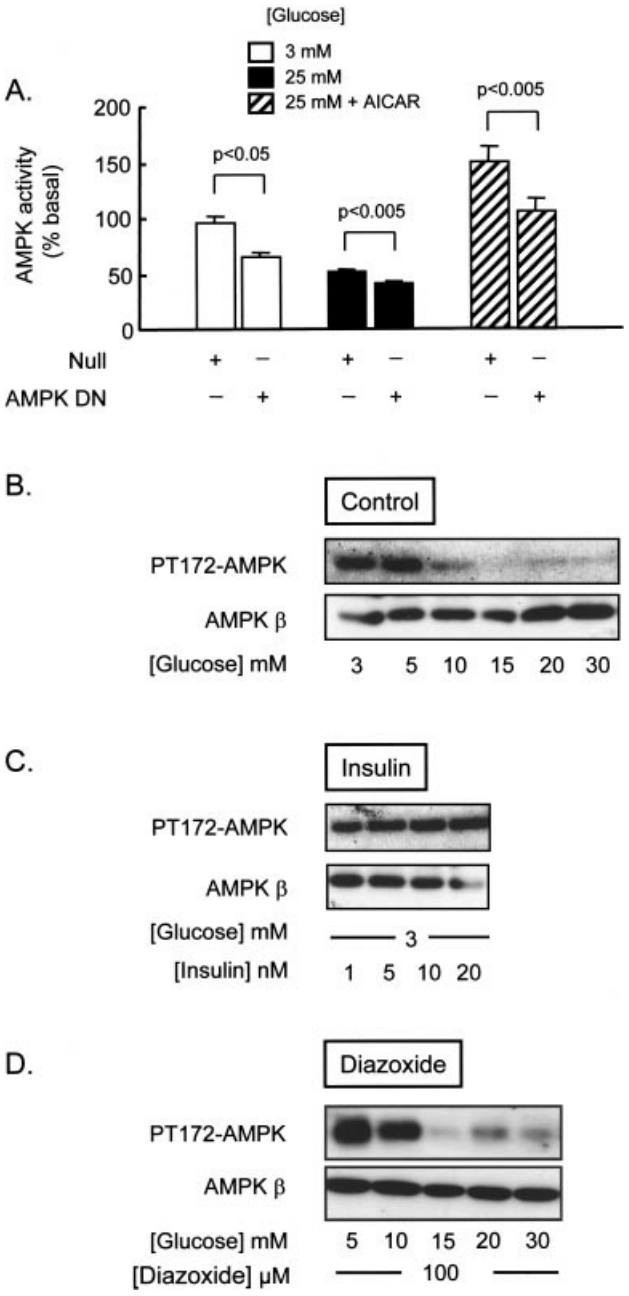

Figure 2 Effects of [glucose] and other agents on AMPK activity and phosphorylation at Thr-172 in MIN6 cells

(**A**) Cells were infected at an multiplicity of infection of 20–30 plaque-forming units/cell with either null or AMPK DN-encoding adenovirus and maintained for 48 h in medium containing 25 mM glucose, before the glucose concentration was lowered to 3 mM for a further 16 h. Cells were then washed once in PBS and incubated in KRB buffer containing 3 mM glucose (white bars), 25 mM glucose (black bars) or 25 mM glucose supplemented with 1 mM AICAR (hatched bars) for 60 min before protein extraction and AMPK assay using SAMS peptide (using synthetic peptide HMRSAMSGLHLVKRR; see the Materials and methods section). Results are expressed as means ± S.E.M. from four independent experiments. (**B**–**D**) MIN6 cells were incubated at the given concentrations of glucose, exogenous insulin or diazoxide, for 1 h as above after overnight incubation at 3 mM glucose. Cell lysis, analysis on SDS/PAGE and immunoblotting were performed as described in the Materials and methods section. Blots were probed using sheep anti-PT-172 antibody (1:1000 dilution; recognizing AMPK phosphorylated at Thr-172) and then stripped and re-probed to reveal total AMPK with a polyclonal anti-AMPK β antibody (1:5000 dilution). Following overnight incubation with the primary antibodies at 4 °C, immunostaining was revealed with horseradish peroxidase conjugated to anti-sheep (1:5000) or anti-rabbit (1:50000) IgG using an enhanced chemiluminescence system (see the Materials and methods section).

This effect was maximal at concentrations of AICAR of 200 μM or above. Addition of 200 μM AICAR to MIN6 cells (Figure 3B), or 400 μM AICAR to isolated rat islets (Figure 3C), led to an essentially complete inactivation of glucose-stimulated insulin release assayed during a 20 min incubation.

To confirm that the effects of AICAR were likely to be due to the activation of AMPK, rather than to potential non-specific effects of this agent (e.g. changes in intracellular adenine nucleotide levels or inhibition of adenosine transport) [49], we next generated adenoviral vectors to explore the effects of active or inactive forms of AMPKα1. Expressed in MIN6 cells at an optimal multiplicity of infection ($\approx$ 30 infectious units/cell or above), each adenovirus led to $> 90\%$ transduction of MIN6 cells (as assessed through the expression of eGFP) and the synthesis of c-Myc-tagged proteins at the molecular masses predicted for AMPK CA (31 kDa) or AMPK DN (63 kDa) [13] (Figure 3D). In common with the effect of AICAR, expression of AMPK CA led to an essentially complete suppression of insulin secretion from MIN6 cells (Figure 3E) at 30 mM glucose, or islets at 16 mM glucose (Figure 3G), while having no significant effect on insulin release at 3 mM glucose in either case. Conversely, infection with AMPK DN led to the activation of insulin secretion at 3 mM glucose, while having no effect on release at 30 mM glucose (Figure 3E). Similarly, the expression of AMPK DN caused a marked stimulation of insulin secretion from rat islets at 3 mM, but not at 16 mM glucose (Figure 3F).

Effects of active and inactive AMPK on glucose metabolism in MIN6 cells

Glucose metabolism was assessed in MIN6 cells expressing constructs encoding either AMPK CA or AMPK DN (Figure 4). Expression of neither construct significantly affected total cellular ATP content in cells incubated at 3.0 mM glucose (Table 1). However, whereas incubation at 30 mM (versus 3.0 mM) glucose for 1 h resulted in a significant increase in total ATP content in cells infected with null adenovirus, or adenovirus encoding AMPK DN, no such increases were evident in AMPK CA-expressing cells (Table 1). Correspondingly, glucose-induced increases in mitochondrial oxidative metabolism, as monitored by changes in cellular autofluorescence (largely due to reduced nicotinamide nucleotides in the mitochondrial matrix) [32], were almost completely suppressed by expression of AMPK CA (Figure 4A). Similarly, AMPK CA expression completely blocked the ability of elevated glucose concentrations to increase the free concentration of ATP, assessed in the mitochondrial matrix ($[ATP]_{mit}$) by expression of a mitochondrially targeted recombinant firefly luciferase [4,32,48,50] (Figure 4C). Moreover, generation of ATP by the glycolytic breakdown of glucose was apparently also completely suppressed, since 30 mM glucose failed to increase cytosolic free [ATP] ($[ATP]_{cyt}$), measured with untargeted firefly luciferase (Figure 4E) [4]. By contrast, expression of AMPK DN had no effect on any of the above metabolic parameters (Figures 4B, 4D and 4F).

Each of the above measurements was performed 16–24 h after the introduction of plasmids encoding AMPK CA or AMPK DN. To explore the possibility that the effects of active or inactive AMPK may therefore result in part or in whole from changes in the expression of key glucose-sensing genes (e.g. GLUT2, glucokinase or L-type pyruvate kinase) [10,37], we next tested the effects of AICAR on glucose-induced increases in mitochondrial or cytosolic free [ATP]. Added 2 min after the achievement of steady-state levels at 30 mM glucose, 200 μM AICAR reduced $[ATP]_{cyt}$ or $[ATP]_{mit}$ by $> 60\%$ (Figures 4G and 4H) within 1 min.

© 2003 Biochemical Society

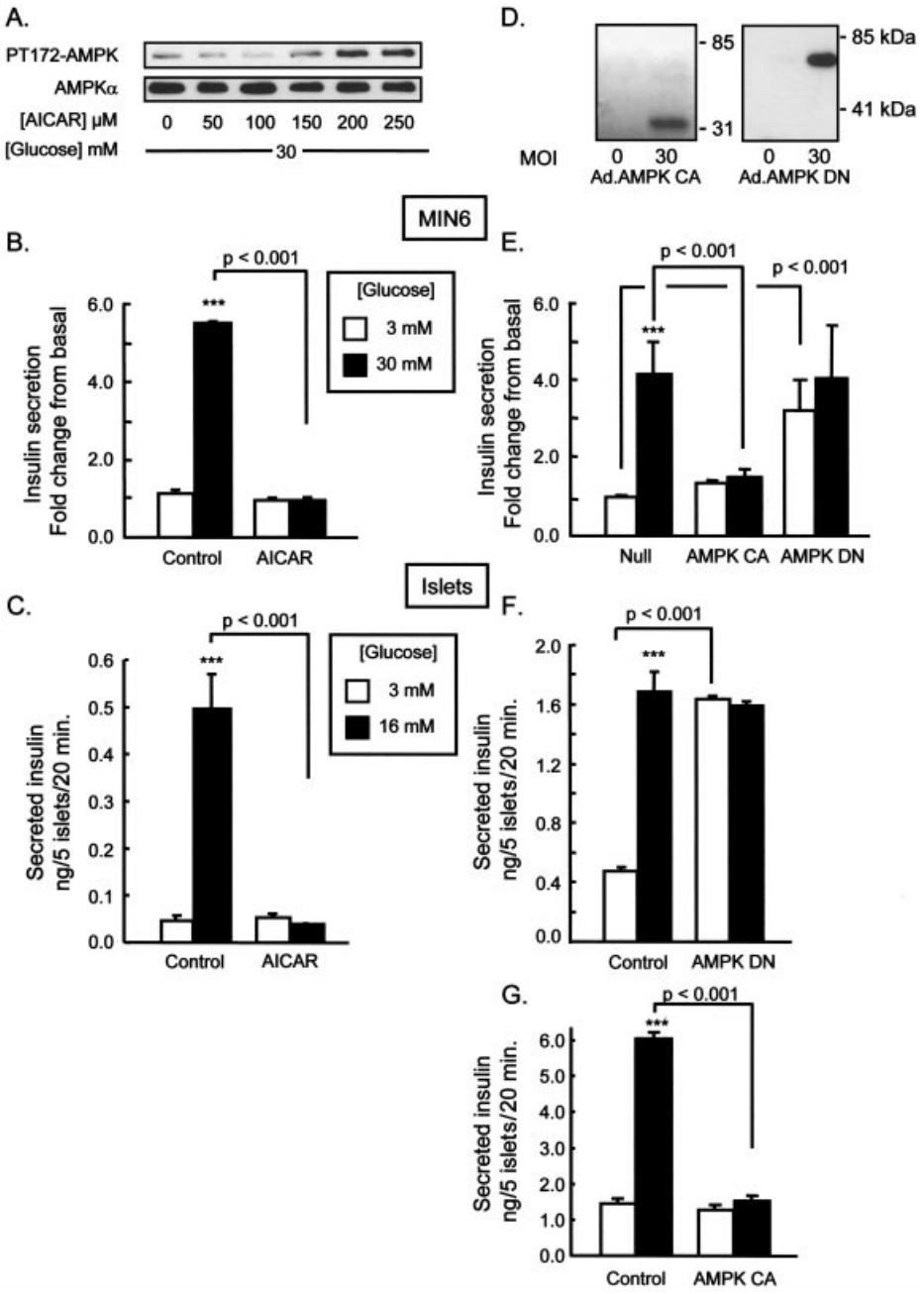

Figure 3 Effect of AMPK activation on glucose-stimulated insulin secretion

(**A**) MIN6 cells were incubated as described in Figure 2 for 60 min at the indicated concentrations of glucose and AICAR, prior to cell lysis and immunoblotting with anti-PT-172 antibody as described in Figure 2. Total AMPK was revealed with rabbit pan-anti-AMPKα antibody (Upstate Biotechnologies; 1:4000 dilution). (**B**) Insulin secretion was measured during incubation of cells for 20 min in KRB medium supplemented with the indicated glucose concentrations in the presence or absence of 200 μM AICAR, as shown. Total and released insulin were quantified by radioimmunoassay, as described in the Materials and methods section. (**C**) Isolated rat islets were cultured for 24 h, prior to measurement of insulin release during 20 min incubation at the indicated glucose concentration, in the presence or absence of 400 μM AICAR. (**D**) MIN6 cells were infected with the indicated viruses at a multiplicity of infection (MOI) of 30 infectious units/cell, prior to cell lysis, SDS/PAGE and immunoblotting with anti-Myc monoclonal antibody (Roche Diagnostics; 1:100 dilution). (**E**) Insulin secretion was measured as in (**B**), from MIN6 cells previously infected with the indicated adenoviruses (see the Materials and methods section). (**F**) Islets were infected with AMPK DN and insulin secretion was measured as in (**C**). (**G**) was as (**F**), but with AMPK CA. $^{***}P < 0.001$ for the effects of the indicated glucose concentrations.

Effects of active and inactive AMPK on $[Ca^{2+}]_c$

Given the effects of AMPK CA and AICAR on glucose-induced insulin secretion (Figure 3) and oxidative metabolism of glucose (Table 1, Figure 4), we predicted that these agents should also suppress glucose-induced increases in intracellular $[Ca^{2+}]_c$ [51,52]. Correspondingly, measured with the trappable intracellular fluorescent probe, fura-2 [53], increases in $[Ca^{2+}]_c$ evoked by 30 mM glucose were inhibited markedly by either AICAR ($> 90\%$) or expression of AMPK CA ($\approx 75\%$; Figure 5A), whereas expression of AMPK DN had no significant effect on glucose-induced $[Ca^{2+}]_c$ changes (Figure 5A).

© 2003 Biochemical Society

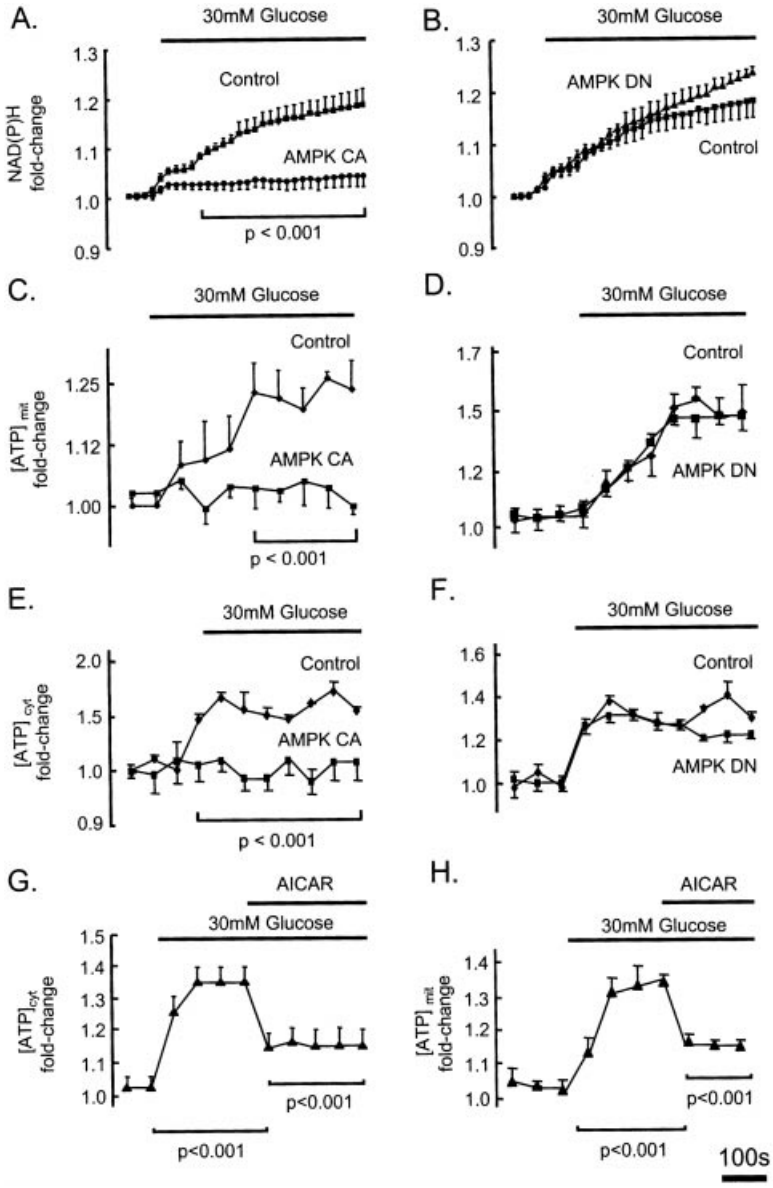

Figure 4 Effect of AICAR, AMPK CA or AMPK DN on glucose-induced changes in oxidative glucose metabolism

(**A**, **B**) MIN6 cells were microinjected with the indicated expression plasmids, plus plasmid pEGFP.N1 (Clontech), or with pEGFP1.N1 alone (10 μg · ml^{-1}), and cultured for 24 h at 25 mM glucose and then 16 h at 3 mM glucose. Autofluorescence due to NAD(P)H was measured over the surface of single cells at 37 °C in modified KRB medium initially containing 3 mM glucose, as described in the Materials and methods section. (**C**, **D**) Cells were microinjected with plasmid pCMV.mitoLuc$_{FF}$ (10 μg · ml^{-1}) plus empty pcDNA3, or the indicated AMPK expression vectors (10 μg · ml^{-1}) and cultured for 24 h at 25 mM glucose and then 16–24 h at 3 mM glucose. Changes in [ATP]$_{mit}$ were measured by luminescence imaging as described in [4,32], in medium initially containing 3 mM glucose. (**E**, **F**) as (**C**, **D**) but after microinjection of expression constructs for untargeted (cytosolic) firefly luciferases. (**G**, **H**) Cells were microinjected with either pCMV.mitoLuc$_{FF}$ or pCMV.Luc$_{FF}$ prior to culture and imaging as described above (**B**–**H**). AICAR (200 μM) was added at the indicated time points. Values of *P* show statistical significance with respect to the control condition (**A**–**F**) or to the preceding time points (**G**, **H**), for five individual cells/condition from separate cultures (**A**, **B**) or 30–60 cells from three different cultures (**C**–**F**).

To determine whether the above effects of AICAR and AMPK CA may be due solely to the effects of these agents on glucose metabolism (Figure 4), we next examined their effects on $[Ca^{2+}]_c$ increases elicited independently of glucose metabolism, through the actions of the sulphonylurea, tolbutamide (Figure 5B). By closing ATP-sensitive K^+ channels, this agent leads to cell depolarization [1] and stimulates Ca^{2+} influx through voltage-gated Ca^{2+} channels [7]. Addition of tolbutamide caused a rapid, partly transient increase in $[Ca^{2+}]_c$, which peaked approx. 30 s after the addition of the drug (Figure 5B). AICAR (200 μM) reduced the peak height of the tolbutamide-induced $[Ca^{2+}]_c$ increases by $\approx 65\%$, and completely eliminated the sustained phase of the $[Ca^{2+}]_c$ increase. Similarly, expression of AMPK CA reduced both the peak and sustained phases, although slightly less markedly (35 and 55 %, respectively). Expression of AMPK DN had no effect on $[Ca^{2+}]_c$ increases in response to tolbutamide (Figure 5B).

To assess the effects of forced changes in AMPK activity on tolbutamide-induced secretion, we next monitored the release of co-expressed hGH, a convenient surrogate which is co-sorted and secreted with insulin in β-cell lines [54]. hGH secretion was stimulated $\approx$ 4.0-fold by either 30 mM (versus 3 mM) glucose

© 2003 Biochemical Society

Table 1 Total cellular ATP content of MIN6 cells

Cells ($\approx$ 300 000) were infected with the indicated viruses and maintained for 16 h at 3.0 mM glucose prior to culture for a further 1 h at the indicated glucose concentrations. Cells were rinsed once in ice-cold PBS, and then extracted in perchloric acid as described in the Materials and methods section, for an assay of total ATP. Data are the means $\pm$ S.E.M. from observations on three separate cell cultures.

[Glucose] (mM)	Adenovirus	Total ATP content (fmol/300 000 cells)
3.0	Null	1017 $\pm$ 7.0
30.0	Null	1323 $\pm$ 3.0*
3.0	AMPK CA	1016 $\pm$ 18.0
30.0	AMPK CA	1019 $\pm$ 14.0†
3.0	AMPK DN	1018 $\pm$ 5.0
30.0	AMPK DN	1322 $\pm$ 8.0*

* $P < 0.001$ for the effect of 30 versus 3.0 mM glucose.
† $P < 0.001$ for the effect of AMPK CA versus null adenovirus.

and 10 μM tolbutamide (Figure 5C). Whereas AMPK CA inhibited the secretion of hGH by more than 95 % (Figure 5C), in common with the effects of this construct on insulin release (Figure 3E), tolbutamide-induced hGH secretion was inhibited by approx. 50 %. Co-expression of AMPK DN had no effect on hGH release provoked by either 30 mM glucose or tolbutamide (Figure 5C).

Effects of active and inactive AMPK on cell viability and apoptosis

One possible explanation for the effects on insulin secretion of overexpression or suppression of AMPK activity might be non-specific actions on cell viability, since increases in AMPK activity have recently been reported to prompt apoptosis in some cell systems [55], while inhibiting apoptosis in others [56,57]. By contrast, in MIN6 cells, expression of neither constitutively active nor dominant-negative forms of AMPK for 24 h had any significant effect on the proportion of apoptotic cells, as judged by the appearance of phosphatidylserine on the outer surface of the plasma membrane (see Figure 6). Moreover, expression of AMPK DN failed to cause any release of *R. reniformis* luciferase into the medium, expressed from a co-transfected plasmid, above that observed after co-transfection with empty vector alone (2.9 and 0.9 % of total *R. reniformis* luciferase activity released/30 min in vector alone or AMPK DN-expressing cells, respectively; means from duplicate determinations). Together, these data argue against an action of elevated or suppressed AMPK activity via non-specific changes in cell viability or plasma membrane integrity.

To further explore this point, we monitored the ability of hormones normally capable of suppressing insulin secretion through the activation of cell-surface, G-protein-coupled receptors, to affect hormone secretion after overexpression of active or inactive forms of AMPK. As anticipated, either somatostatin (Figure 7A) or the α2-adrenoreceptor agonist clonidine [58] (Figure 7B) completely blocked the release of transfected hGH elicited by 30 mM glucose, or release stimulated by co-transfection with AMPK DN. Neither agent exerted any detectable effect on hGH release at 3 mM glucose, nor release at 3 or 30 mM glucose in cells co-transfected with AMPK CA (Figures 7A and 7B).

Each of the above receptor agonists is likely to inhibit insulin (and transfected hGH) release through actions both to decrease intracellular $[Ca^{2+}]_c$ [58], and at a late exocytotic step [59]. By contrast, the K_{ATP} channel opener diazoxide [5] is predicted to act largely by hyperpolarizing the cell, thus suppressing $[Ca^{2+}]_c$ increases. Whereas 100 μM diazoxide completely inhibited glucose-stimulated hGH release (Figure 7C), this drug was without effect on the release of hGH stimulated by co-expression of dominant-negative AMPK (Figure 7C).

Role of changes in ACC phosphorylation in the regulation of insulin secretion by active and inactive AMPK

The activity of ACC I, the predominant isoform of this enzyme in β-cells [23], has previously been shown to be reduced acutely by incubation of INS-1 β-cells at elevated glucose concentrations [23]. Glucose-induced increases in ACC I activity, which could be reversed by AICAR, were ascribed to dephosphorylation of Ser-79 in the regulatory domain [23,60]. Correspondingly, use of a phospho-specific antibody revealed that the phosphorylation of ACC I on Ser-79 was reduced by 40–60 % in MIN6 cells incubated for 1 h at 25 or 30 versus 3 mM glucose, in concert with the inhibition of AMPK phosphorylation at Thr-172 (Figures 8A–8C). AICAR increased ACC I phosphorylation at Ser-79 dose-dependently (Figure 8B) and, at 200 μM, increased phosphorylation at this site at both 3 and 30 mM glucose (Figure 8C). By contrast, expression of AMPK DN significantly decreased the extent of phosphorylation of ACC I at 3 or 30 mM glucose, as monitored in single cells co-transfected with AMPK DN-encoding plasmid (Figure 8D).

The above results thus provide correlative evidence that changes in ACC I activity may be involved in the stimulation of insulin release by glucose. As proposed by Corkey, Prentki and co-workers [61], increases in ACC I activity in response to elevated glucose concentrations, as a result of dephosphorylation of Ser-79 (Figures 8A and 8B) [23,60], may also elevate intracellular malonyl-CoA levels. The consequent inhibition of mitochondrial carnitine palmitoyltransferase I, and thus β-oxidation, may then increase intracellular acyl-CoA concentrations, as has previously been reported in islets perfused at elevated glucose concentrations [62]. In MIN6 cells, 30 mM glucose caused a 2.5-fold increase in intracellular malonyl-CoA levels, an effect which was progressively reversed by increasing concentrations of AICAR (Figure 9A). Consistent with the view that AICAR acted principally to increase AMPK activity, transduction of MIN6 cells with AMPK CA adenovirus also suppressed completely glucose-induced increases in [malonyl-CoA] (Figure 9B). By contrast, malonyl-CoA levels at 3 and 30 mM glucose in cells transduced with adenovirus encoding AMPK DN were indistinguishable from those in null-virus-treated cells (Figure 9B).

DISCUSSION

Regulation of PPI gene expression by glucose, insulin and AMPK

Through the use of molecular tools (dominant-positive and -negative forms of AMPK) the present study reinforces recent findings on the regulation of PPI gene expression [10]. In these earlier studies, PPI promoter activity was found to be regulated reciprocally by AICAR, which inhibited activity, and by intracellular microinjection of antibodies to AMPKα2, which stimulated the promoter at low glucose concentrations. Moreover, PPI promoter activity was also found in other studies to be regulated by glucose largely through the action of released insulin, in MIN6 cells [43] as well as in HIT-T15 and primary β-cells [45]. The present work draws these observations together by

© 2003 Biochemical Society

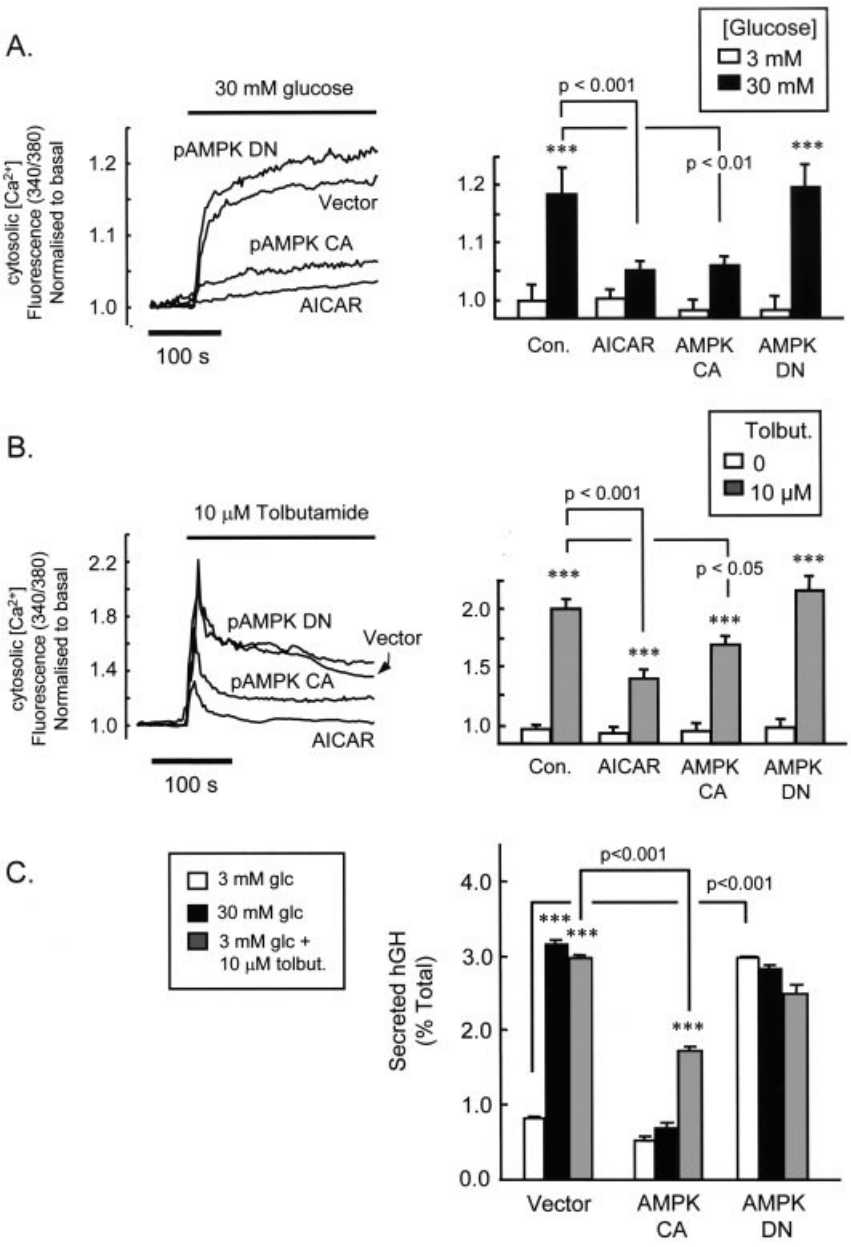

Figure 5 Effects of AMPK CA and AMPK DN on glucose and tolbutamide-induced increases in $[Ca^{2+}]_c$

(**A**) Changes in intracellular free $[Ca^{2+}]$ provoked by 30 versus 3 mM glucose were measured using fura-2 in cells co-microinjected with either empty vector, or the AMPK expression vectors indicated, plus plasmid pEGFP.N1, and cultured for 24 h at 25 mM glucose, then 16 h at 3 mM glucose. $[Ca^{2+}]_c$ was monitored in real time in 5–12 single cells/condition by monitoring changes in fura-2 fluorescence ratio at an acquisition rate of 1.0 data points/s (see the Materials and methods section). (**B**) as (**A**) but during stimulation with 10 μM tolbutamide (Tolbut.). (**C**) Cells were co-transfected with pcDNA3.hGH plus empty pcDNA3 (Vector) or with pcDNA3 plus the indicated AMPK expression constructs. After culture at 25 and 3 mM glucose as in (**A**), cells were incubated for 20 min in KRB medium supplemented with additions as indicated. Total and released hGH were measured by ELISA (see the Materials and methods section).

demonstrating that the effects of changes in AMPK activity (Figure 1) are likely to be mediated in large part, though not exclusively, by changes in the rate of insulin secretion (Figures 3 and 10). However, it should be stressed that the inability of exogenous insulin to completely restore PPI promoter activity in AMPK CA-expressing cells (Figure 1A) does suggest that activated AMPK may affect PPI gene expression through additional, insulin-independent mechanisms. These may include alterations in the stability or transactivation capacity of key transcription factors [37] or decreases in intracellular malonyl-CoA (Figure 9), and consequently acyl-CoA, levels [63].

Effects of forced increases in AMPK activity on glucose-stimulated insulin secretion

In agreement with two previous reports [22,23], AICAR treatment is shown to reverse the acute stimulation of insulin release by glucose both in a clonal β-cell line (Figure 3E) and in primary

© 2003 Biochemical Society

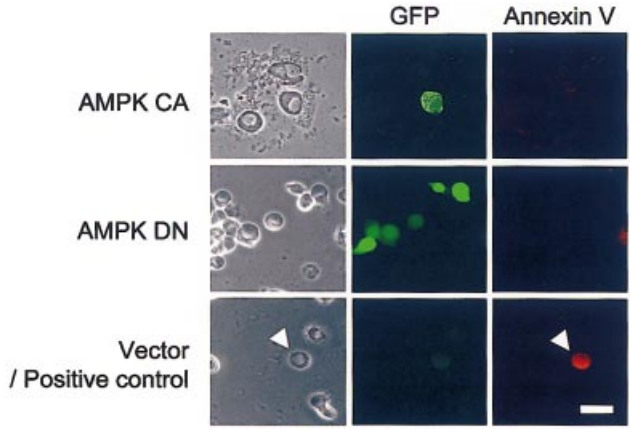

Figure 6 Effect of AMPK CA and AMPK DN on apoptosis in MIN6 cells

Cells were transfected with the expression constructs pAdTrack.CMV.AMPK CA (upper panels) or pAdTrack.CMV.AMPK DN (middle panels) or empty vector (pAdTrack.CMV; lower panels). The level of apoptosis was measured in transfected cells (identified through eGFP fluorescence) by labelling with FITC-tagged annexin V (right-hand panels). Note the presence of an apoptotic cell (arrowhead) after transfection with eGFP alone (Vector/Positive control). Numbers of apoptotic cells were 1 in 150, 0 in 130 and 5 in 346 cells respectively, analysed in three independent experiments after transfection with AMPK CA-expressing, AMPK DN-expressing or empty vector alone. Scale bar, 50 μm.

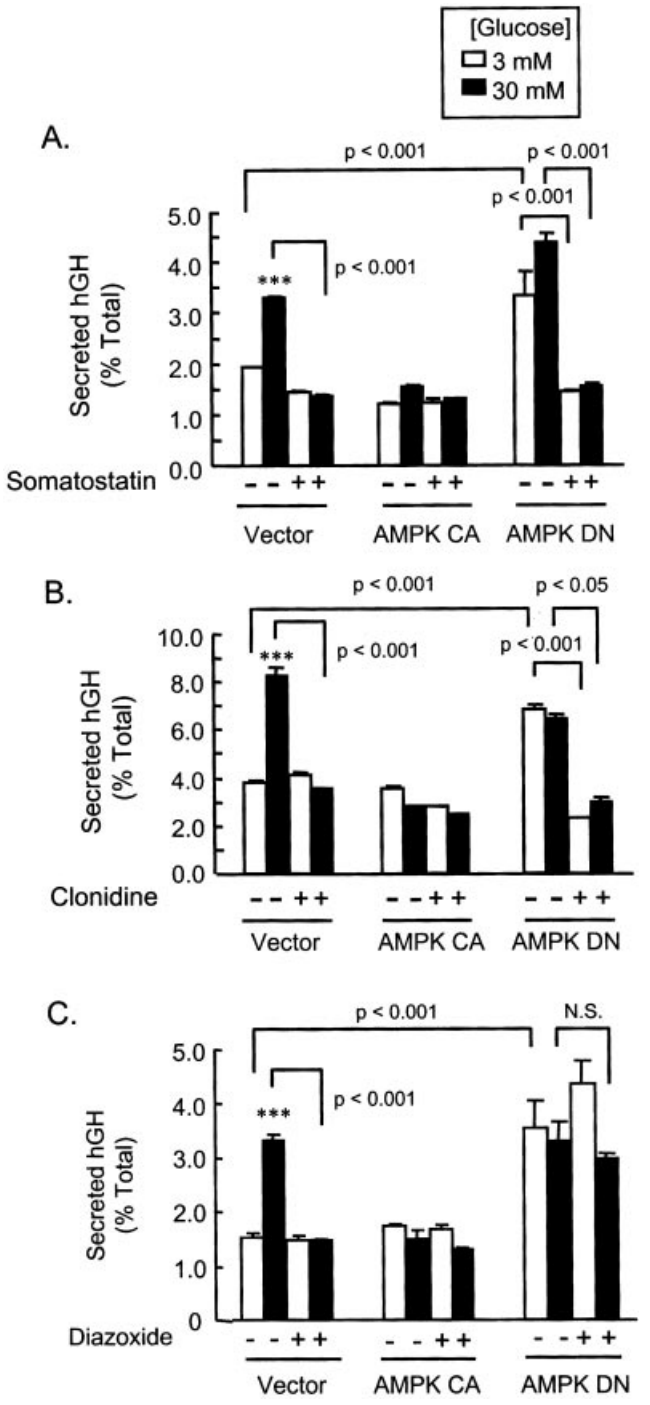

Figure 7 Regulation of hGH release by somatostatin, clonidine and diazoxide

Cells were co-transfected with pCMV.hGH plus empty pcDNA3 (Vector), pcDNA3.AMPK CA or pcDNA3.AMPK DN, as indicated, before culture at 25 and 3 mM glucose, as described in Figure 3. Total cellular hGH, and hGH released during 30 min incubation in modified KRB medium containing the indicated additions, were measured by ELISA. Where present, the concentrations of somatostatin, clonidine and diazoxide were 100, 10 and 100 μM, respectively. N.S., not significant.

rat islets (Figure 3C). However, as reported by Salt and colleagues [22] and by other workers [24], we did notice a tendency for this agent to enhance basal insulin release at low glucose concentrations from islets (Figure 3C), but not MIN6 cells.

We now extend these findings with the important observation that the activation of AMPK, achieved through adenovirus-mediated expression of a constitutively active form of the enzyme, is likely to be the chief mechanism responsible for the effects of AICAR (Figure 3C). Furthermore, we explore in detail the mechanism(s) through which the activation of AMPK may suppress insulin release (Figures 3–5). Unexpectedly, expression of active AMPK is shown to dramatically decrease the oxidative metabolism of glucose (Figure 4), and almost completely abolish glucose-induced $[Ca^{2+}]_c$ increases (Figure 5A). Interestingly, the effects of activated AMPK on glucose-induced increases in mitochondrial and cytosolic [ATP] were only partly mimicked by AICAR (Figures 4C and 4E versus 4G and 4H). Thus sustained activation of AMPK, as achieved by overexpression of AMPK CA, may lead to the changes in expression of glucose-sensing enzymes (e.g. a decrease in the levels of GLUT2, glucokinase or L-type pyruvate kinase [10,37,64] or an increase in lactate dehydrogenase [32,65] or plasma-membrane monocarboxylate transporter [66] activities). Such changes may act in concert with alterations in the phosphorylation state of key metabolic enzymes (see below) to impede the normal metabolism of glucose and hence the triggering of insulin secretion.

Furthermore, either AICAR treatment or constitutive expression of active AMPK caused a sharp reduction in metabolism-independent $[Ca^{2+}]_c$ elicited by tolbutamide (Figure 5B), and these were closely paralleled by decreases in hormone release (Figure 5C). The simplest explanation of the latter findings is that active AMPK is capable of either inhibiting a Ca^{2+} channel, or activating a Ca^{2+} pump, in β-cells (see Figure 10).

Since the likely metabolic targets for AMPK in the β-cell are not fully defined, the mechanisms by which AICAR or AMPK CA may inhibit glucose metabolism must remain a matter for speculation. Nevertheless, phosphorylation of ACC I, and corresponding decreases in intracellular malonyl-CoA concentration (Figures 9A and 9B), and thus enhanced acyl-CoA oxidation,

© 2003 Biochemical Society

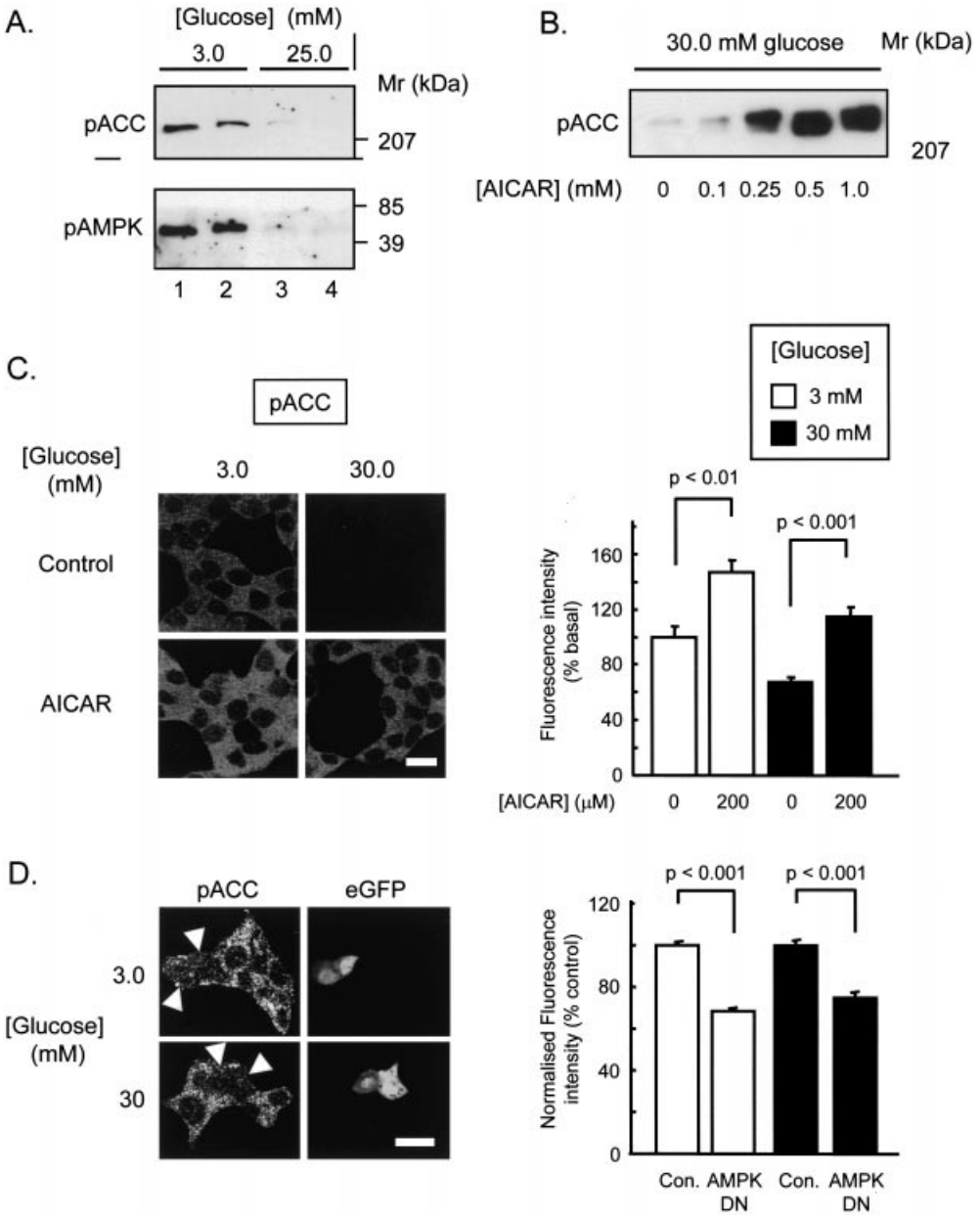

Figure 8 Effect of glucose, AICAR and AMPK DN on ACC I phosphorylation at Ser-79

(**A**) MIN6 cells were cultured for 16 h in medium containing 3 mM glucose and then for 1 h in KRB containing either 3 or 25 mM glucose as indicated. Cells were then extracted into lysis buffer, and extracts (equivalent to 30 μg of protein) subjected to SDS/PAGE and Western analysis (see the Materials and methods section) of ACC I phosphorylation at Ser-79 (upper panel, lanes 1 and 2) or AMPK phosphorylation at Thr-172 (lower panel, lanes 3 and 4). Even loading in each lane was verified by staining with Ponceau Red. (**B**) Dose response to AICAR of ACC I Ser-79 phosphorylation at 30 mM glucose: other incubation conditions were as in (**A**). In (**C**) MIN6 cells were cultured at 25 mM glucose for 24 h and then incubated in modified KRB for 1 h at the indicated glucose concentrations in the presence or absence of 200 μM AICAR. Cells were then fixed and stained with a rabbit polyclonal anti-(ACC I phospho-Ser-79) antibody (1:50) and visualized with an Alexa 568 goat anti-rabbit (1:500) secondary antibody (568 nm excitation and tetramethylrhodamine isothiocyanate filters for emission). In (**C**), images were captured on a Leica TCS-NT confocal laser-scanning microscope keeping the laser power and all imaging parameters constant throughout. The fluorescence intensity of ACC I immunostaining was quantified in groups of cells with the Leica software, and compared with values obtained at 3 mM glucose. Mean $\pm$ S.E.M. fluorescence data represent five randomly selected groups of cells in three independent experiments. (**D**) Cells were co-transfected with plasmid pAdTrack.AMPK DN and 24 h later AMPK DN-expressing cells were identified by exciting eGFP at 488 nm and using FITC filters for fluorescence emission (right-hand panels). The same cells were immunostained with a rabbit polyclonal anti-(ACC1 phospho-Ser-79) antibody (left-hand panels) as described above. Arrowheads indicate the positions of transfected cells. The fluorescence intensity of ACC I immunostaining in AMPK DN-expressing cells was measured and normalized to that of neighbouring cells in the same field. Mean $\pm$ S.E.M. fluorescence data were obtained from 14 AMPK DN-expressing and 27 control cells at 30 mM glucose and 3 AMPK DN-expressing and 3 control cells at 3 mM glucose. Scale bars, 20 μm. Blots shown in (**A**–**C**) are representative of three independent experiments.

may be predicted to suppress glucose metabolism through the operation of a β-cell 'Randle cycle' [67]. In this context, it should also be noted that inhibition of mitochondrial pyruvate oxidation leads to a complete suppression of glycolytic flux and hence of glucose utilization in the β-cell, since pyruvate cannot be converted efficiently into lactate in these cells [32,65,68,69]. Such a

© 2003 Biochemical Society

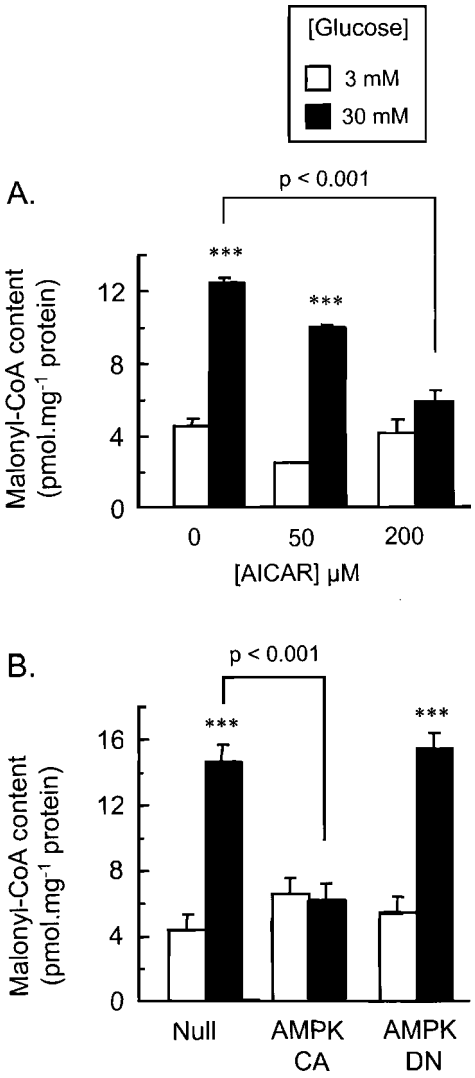

Figure 9 Regulation of intracellular malonyl-CoA levels by glucose, AICAR, AMPK CA and AMPK DN

(**A**) MIN6 cells were grown to confluence in 25 cm^2 flasks in medium containing 3 mM glucose for 16 h prior to extraction. Cells were then incubated in modified KRB medium at the indicated glucose concentrations, and in the absence or presence of 50 or 200 μM AICAR, for 20 min at 37 °C. Malonyl-CoA content was assayed as described in the Materials and methods section. (**B**) MIN6 cells were infected with the indicated adenoviruses, prior to incubation as in (**A**), and quantitation of cellular malonyl-CoA content.

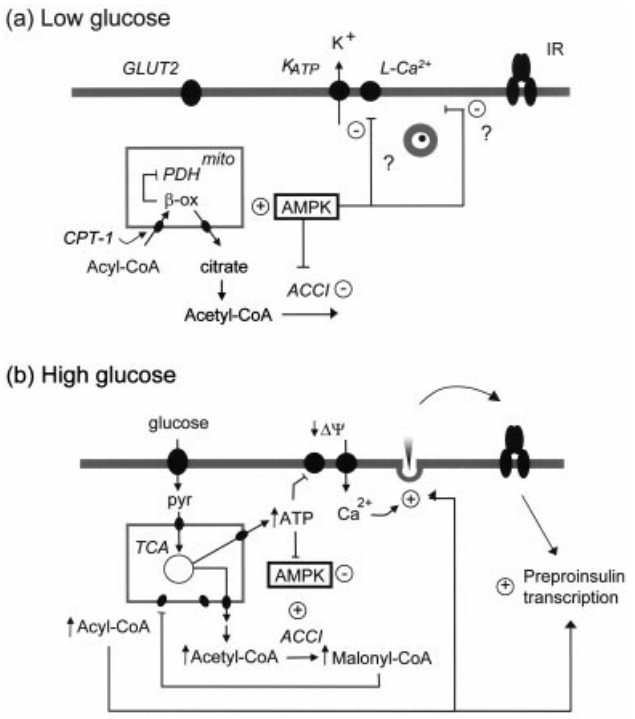

Figure 10 Possible roles of AMPK in the control of insulin release and PPI gene expression

At low glucose concentrations (**a**), active AMPK inhibits glucose-dependent ATP production, possibly (but not exclusively) through inactivation of ACC I, and blockade of malonyl-CoA synthesis. AMPK also suppresses Ca^{2+} influx and/or Ca^{2+} extrusion from the cytosol, by presently undefined mechanisms, and blocks a late (Ca^{2+}-independent) step in exocytosis. An increase in glucose concentration (**b**) leads progressively to the inhibition of AMPK activity, de-inhibiting ATP production and leading to the closure of K_{ATP} channels. Inhibition of AMPK also leads to de-inhibition of ACC I, which is essential to permit an increase in malonyl-CoA synthesis. Inhibition of carnitine palmitoyltransferase I (CPT1) leads to decreased β-oxidation (β-ox) of fatty acids (thus permitting more rapid pyruvate oxidation) and also permits the accumulation of acyl-CoA in the cytosol. Acyl-CoA may then stimulate late events in vesicle fusion at the plasma membrane. Released insulin may then activate β-cell insulin receptors leading, along with increases in intracellular [acyl-CoA], to the induction of PPI gene transcription. PDH^{mito}, pyruvate dehydrogenase of the mitochondrial compartment; L-Ca^{2+}, L-type calcium channel; Pyr, pyruvate; TCA, tricarboxylate; IR, insulin receptor; $\Delta\Psi$, membrane potential.

mechanism may, therefore, underline the inhibition of glucose-induced increases in total ATP (Table 1) as well as mitochondrial and cytosolic free [ATP] in cells expressing active AMPK (Figures 4C and 4E) or treated acutely with AICAR (Figures 4G and 4H).

Effects of AMPK DN on glucose-stimulated insulin release

An intriguing finding made during these studies is that inhibition of AMPK activity with a dominant-negative form of the enzyme, expected to inhibit both AMPKα1 and α2 complexes [29], leads to the activation of insulin secretion by mechanisms that are at least partly distinct from those which mediate the effects of glucose (Figures 4, 5 and 7). Thus expression of AMPK DN had no apparent effect on the stimulation of ATP synthesis by glucose (Figures 4B, 4D and 4F), nor on intracellular Ca^{2+} concentrations (Figures 5A and 5B). It therefore follows that inhibition of AMPK by glucose is not in itself sufficient to close K_{ATP} channels, nor to prompt Ca^{2+} influx. On the other hand, suppression of AMPK activity did stimulate profoundly the secretion of insulin or transfected hGH (Figures 3E and 5C, respectively), and these effects were resistant to the hyperpolarizing action of diazoxide (Figure 7C, and results not shown). What may underlie this stimulation of secretion upon inhibition of AMPK? Importantly, measurements of apoptosis (Figure 6), of cellular protein release (see Results), and of preserved somatostatin or α2-adrenoreceptor-mediated inhibition of secretion (Figures 7B and 7C), would appear to rule out non-specific alterations in cell viability in cells in which AMPK is inactivated.

We therefore explored the possibility that a decrease in the level of phosphorylation of ACC at Ser-79, and hence an increase in cellular malonyl-CoA synthesis, may prompt the release of insulin through a Ca^{2+}-independent mechanism involving an increase in cellular acyl-CoA concentration, as described previously in permeabilized HIT-T15 cells [70]. However, arguing against this model, the decreased phosphorylation of ACC

© 2003 Biochemical Society

elicited by AMPK DN (Figure 8D) failed to lead to any increase in intracellular [malonyl-CoA] at either low or high glucose concentrations (Figure 9B). This observation would appear to indicate that other factors, including substrate supply, may be of greater importance for regulating flux through ACC I in intact β-cells when ACC is largely in the active, dephosphorylated form.

Instead, we speculate that the expression of AMPK DN leads, either directly or indirectly, to the dephosphorylation of an undefined target protein, thus activating insulin release through a novel, Ca^{2+}-independent mechanism. Future studies will be required to identify this target, and its mechanism of action.

Conclusion

We propose (Figure 10) that (i) AMPK acts as a pleiotropic regulator of insulin secretion in pancreatic β-cells and that (ii) inhibition of AMPK is required, but not sufficient, for the normal triggering of insulin release by glucose. An important further consequence of these and earlier observations [22,23] is that *in vivo* administration of AICAR, recently shown to cause improvements in glucose homoeostasis in a number of models of diabetes, including *ob/ob* and *db/db* mice [71] as well as high-fat-fed rats [72], is likely to cause decreases in blood insulin levels both indirectly (due to the fall in plasma glucose concentration) but also through a direct action on the β-cell. Similarly, metformin, a widely used insulin sensitizer, has also very recently been shown to activate AMPK and to suppress gluconeogenesis in isolated liver cells [73], and could thus also inhibit insulin secretion directly. However, it should be stressed that the expression of AMPK catalytic subunit isoforms is different in β-cells ($\alpha1 \gg \alpha2$) [10] than in muscle ($\alpha1 < \alpha2$) [12] or liver cells ($\alpha1 \approx \alpha2$) [29]. Given the existence of other possible differences in the relative abundances of the β- and γ-subtypes in these tissues, isoform-selective activators or inhibitors of AMPK may thus provide new therapeutic tools for the treatment of type 2 diabetes mellitus.

This work was supported by Programme and Project grants from the Wellcome Trust, the Biotechnology and Biological Sciences Research Council, the Human Frontiers Science Program, the Medical Research Council (U.K.) and Diabetes U.K. We thank Dr Mark Jepson and Mr Alan Leard (Bristol MRC Imaging Facility), and Ms Rebecca Rowe for technical assistance. I.L. is a Wellcome Advanced Fellow and G.A.R. is a Wellcome Trust Research Leave Fellow.

REFERENCES

1 Rutter, G. A. (2001) Nutrient-secretion coupling in the pancreatic islet β-cell: recent advances. Mol. Aspects Med. **22**, 247–284
2 Rutter, G. A., Tavaré, J. M. and Palmer, D. G. (2000) Regulation of gene expression by glucose. News Physiol. Sci. **15**, 149–154
3 Webb, G. C., Akbar, M. S., Zhao, C. J. and Steiner, D. F. (2001) Expression profiling of pancreatic β-cells – glucose regulation of secretory and metabolic pathway genes. Diabetes **50**, S135–S136
4 Kennedy, H. J., Pouli, A. E., Jouaville, L. S., Rizzuto, R. and Rutter, G. A. (1999) Glucose-induced ATP microdomains in single islet β-cells. J. Biol. Chem. **274**, 13281–13291
5 Bryan, J. and Aguilar-Bryan, L. (1997) The ABCs of ATP-sensitive potassium channels: more pieces of the puzzle. Curr. Opin. Cell Biol. **9**, 553–559
6 Henquin, J. C. and Meissner, H. P. (1984) Significance of ionic fluxes and changes in membrane potential for stimulus-secretion coupling in pancreatic B-cells. Experientia **40**, 1043–1052
7 Safayhi, H., Haase, H., Kramer, U., Bihlmayer, A., Roenfeldt, M., Ammon, H. P., Froschmayr, M., Cassidy, T. N., Morano, I., Ahlijanian, M. K. and Striessnig, J. (1997) L-type calcium channels in insulin-secreting cells: biochemical characterization and phosphorylation in RINm5F cells. Mol. Endocrinol. **11**, 619–629
8 Melloul, D., Marshak, S. and Cerasi, E. (2002) Regulation of insulin gene transcription. Diabetologia **45**, 309–326
9 Leclerc, I., da Silva Xavier, G. and Rutter, G. A. (2002) AMP- and stress activated protein kinases: key regulators of gene transcription in mammalian cells. Progr. Nucleic Acid Res. Mol. Biol. **71**, 69–90
10 da Silva Xavier, G., Leclerc, I., Salt, I. P., Doiron, B., Hardie, D. G., Kahn, A. and Rutter, G. A. (2000) Role of AMP-activated protein kinase in the regulation by glucose of islet β-cell gene expression. Proc. Natl. Acad. Sci. U.S.A. **97**, 4023–4028
11 Gao, G., Fernandez, C. S., Stapleton, D., Auster, A. S., Widmer, J., Dyck, J. R., Kemp, B. E. and Witters, L. A. (1996) Non-catalytic β- and γ-subunit isoforms of the 5′-AMP-activated protein kinase. J. Biol. Chem. **271**, 8675–8681
12 Stapleton, D., Mitchelhill, K. I., Gao, G., Widmer, J., Michell, B. J., Teh, T., House, C. M., Fernandez, C. S., Cox, T., Witters, L. A. and Kemp, B. E. (1996) Mammalian AMP-activated protein kinase subfamily. J. Biol. Chem. **271**, 611–614
13 Hardie, D. G., Carling, D. and Carlson, M. (1998) The AMP-activated/SNF1 protein kinase subfamily: metabolic sensors of the eukaryotic cell? Annu. Rev. Biochem. **67**, 821–855
14 Hardie, D. G. and Carling, D. (1997) The AMP-activated protein kinase–fuel gauge of the mammalian cell? Eur. J. Biochem. **246**, 259–273
15 Kemp, B. E., Mitchelhill, K. I., Stapleton, D., Michell, B. J., Chen, Z. P. and Witters, L. A. (1999) Dealing with energy demand: the AMP-activated protein kinase. Trends Biochem. Sci. **24**, 22–25
16 Brown, M. S., Brunschede, G. Y. and Goldstein, J. L. (1975) Inactivation of 3-hydroxy-3-methylglutaryl coenzyme A reductase in vitro. An adenine nucleotide-dependent reaction catalyzed by a factor in human fibroblasts. J. Biol. Chem. **250**, 2502–2509
17 Yeh, L. A., Lee, K. H. and Kim, K. H. (1980) Regulation of rat liver acetyl-CoA carboxylase. Regulation of phosphorylation and inactivation of acetyl-CoA carboxylase by the adenylate energy charge. J. Biol. Chem. **255**, 2308–2314
18 Carling, D., Zammit, V. A. and Hardie, D. G. (1987) A common bicyclic protein kinase cascade inactivates the regulatory enzymes of fatty acid and cholesterol biosynthesis. FEBS Lett. **223**, 217–222
19 Hardie, D. G., Carling, D. and Sim, A. T. R. (1989) The AMP-activated protein kinase: a multisubstrate regulator of lipid metabolism. Trends Biochem. Sci. **14**, 20–23
20 Munday, M. R., Milic, M. R., Takhar, S., Holness, M. J. and Sugden, M. C. (1991) The short-term regulation of hepatic acetyl-CoA carboxylase during starvation and re-feeding in the rat. Biochem. J. **280**, 733–737
21 Stapleton, D., Gao, G., Michell, B. J., Widmer, J., Mitchelhill, K., Teh, T., House, C. M., Witters, L. A. and Kemp, B. E. (1994) Mammalian 5′-AMP-activated protein kinase non-catalytic subunits are homologs of proteins that interact with yeast Snf1 protein kinase. J. Biol. Chem. **269**, 29343–29346
22 Salt, I. P., Johnson, G., Ashcroft, S. J. and Hardie, D. G. (1998) AMP-activated protein kinase is activated by low glucose in cell lines derived from pancreatic β cells, and may regulate insulin release. Biochem. J. **335**, 533–539
23 Zhang, S. and Kim, K. H. (1995) Glucose activation of acetyl-CoA carboxylase in association with insulin secretion in a pancreatic β-cell line. J. Endocrinol. **147**, 33–41
24 Akkan, A. G. and Malaisse, W. J. (1994) Insulinotropic action of AICA riboside. I. Insulin release by isolated islets and the perfused pancreas. Diabetes Res. **25**, 13–23
25 Malaisse, W. J., Conget, I., Sener, A. and Rorsman, P. (1994) Insulinotropic action of AICA riboside. II. Secretory, metabolic and cationic aspects. Diabetes Res. **25**, 25–37
26 Stein, S. C., Woods, A., Jones, N. A., Davison, M. D. and Carling, D. (2000) The regulation of AMP-activated protein kinase by phosphorylation. Biochem. J. **345**, 437–443
27 Sugden, C., Crawford, R. M., Halford, N. G. and Hardie, D. G. (1999) Regulation of spinach SNF1-related (SnRK1) kinases by protein kinases and phosphatases is associated with phosphorylation of the T loop and is regulated by 5′-AMP. Plant J. **19**, 433–439
28 Fisher, R. J. and Burgoyne, R. D. (1999) The effect of transfection with Botulinum neurotoxin C1 light chain on exocytosis measured in cell populations and by single-cell amperometry in PC12 cells. Pflugers Arch. Eur. J. Physiol. **437**, 754–762
29 Woods, A., Azzout-Marniche, D., Foretz, M., Stein, S. C., Lemarchand, P., Ferré, P., Foufelle, F. and Carling, D. (2000) Characterization of the role of AMP-activated protein kinase in the regulation of glucose-activated gene expression using constitutively active and dominant negative forms of the kinase. Mol. Cell. Biol. **20**, 6704–6711
30 Rafiq, I., Kennedy, H. and Rutter, G. A. (1998) Glucose-dependent translocation of insulin promoter factor-1 (IPF-1) between the nuclear periphery and the nucleoplasm of single MIN6 β-cells. J. Biol. Chem. **273**, 23241–23247
31 He, T. C., Zhou, S., da Costa, L. T., Yu, J., Kinzler, K. W. and Vogelstein, B. (1998) A simplified system for generating recombinant adenoviruses. Proc. Natl. Acad. Sci. U.S.A. **95**, 2509–2514
32 Ainscow, E. K., Zhao, C. and Rutter, G. A. (2000) Acute overexpression of lactate dehydrogenase-A perturbs β-cell mitochondrial metabolism and insulin secretion. Diabetes **49**, 1149–1155
33 Miyazaki, J., Araki, K., Yamato, E., Ikegami, H., Asano, T., Shibasaki, Y., Oka, Y. and Yamamura, K. (1990) Establishment of a pancreatic β cell line that retains glucose inducible insulin secretion: special reference to expression of glucose transporter isoforms. Reg. Peptides. **127**, 126–132

© 2003 Biochemical Society

34 Kennedy, H. J., Viollet, B., Rafiq, I., Kahn, A. and Rutter, G. A. (1997) Upstream stimulatory factor-2 (USF2) activity is required for glucose stimulation of L-pyruvate kinase promoter activity in single living islet β-cells. J. Biol. Chem. **272**, 20636–20640

35 Gotoh, M., Maki, T., Kiyoizumi, T., Satomi, S. and Monaco, A. P. (1985) An improved method for isolation of mouse pancreatic islets. Transplantation **40**, 437–438

36 Varadi, A., Molnar, E., Ostenson, C. G. and Ashcroft, S. J. H. (1996) Isoforms of endoplasmic reticulum Ca^{2+}-ATPase are differentially expressed in normal and diabetic islets of Langerhans. Biochem. J. **319**, 521–527

37 Leclerc, I., Lenzner, C., Gourdon, L., Vaulont, S., Kahn, A. and Viollet, B. (2001) Hepatocyte nuclear factor-4α involved in type 1 maturity-onset diabetes of the young is a novel target of AMP-activated protein kinase. Diabetes **50**, 1515–1521

38 Varadi, A. and Rutter, G. A. (2002) Dynamic imaging of endoplasmic reticulum $[Ca^{2+}]$ in MIN6 β-cells using recombinant cameleons: roles of SERCA2 and ryanodine receptors. Diabetes **51**, S190–S201

39 Hughes, R. J. (1983) A bioluminescent assay for glycogen phosphorylase in cultured cells. Anal. Biochem. **131**, 318–323

40 Rutter, G. A., Burnett, P., Rizzuto, R., Brini, M., Pozzan, T., Tavaré, J. M. and Denton, R. M. (1996) Digital imaging of intramitochondrial Ca^{2+} with recombinant targeted aequorin: significance for the regulation of pyruvate dehydrogenase activity. Proc. Natl. Acad. Sci. U.S.A. **93**, 5489–5494

41 Rutter, G. A., Kennedy, H. J., Wood, C. D., White, M. R. H. and Tavaré, J. M. (1998) Quantitative real-time imaging of gene expression in single cells using multiple luciferase reporters. Chem. Biol. **5**, R285–R290

42 Robb-Gaspers, L. D., Burnett, P., Rutter, G. A., Denton, R. M., Rizzuto, R. and Thomas, A. P. (1998) Integrating cytosolic calcium signals into mitochondrial metabolic responses. EMBO J. **17**, 4987–5000

43 daSilvaXavier, G., Varadi, A., Ainscow, E. and Rutter, G. A. (2000) Regulation of gene expression by glucose in pancreatic β-cells (MIN6) via insulin secretion and activation of phosphatidyl inositol 3′ kinase. J. Biol. Chem. **275**, 36269–36277

44 Vlahos, C. J., Matter, W. F., Hui, K. Y. and Brown, R. F. (1994) A specific inhibitor of phosphatidylinositol 3-kinase, 2-(4-morpholinyl)-8-phenyl-4H-1-benzopyran-4-one (LY294002). J. Biol. Chem. **269**, 5241–5248

45 Leibiger, I. B., Leibiger, B., Moede, T. and Berggren, P. O. (1998) Exocytosis of insulin promotes insulin gene transcription via the insulin receptor PI-3 kinase p70 s6 kinase and CaM kinase pathways. Mol. Cell **1**, 933–938

46 Rutter, G. A. (1999) Insulin secretion: Feed-forward control of insulin biosynthesis? Curr. Biol. **9**, R443–R445

47 Detimary, P., Gilon, P. and Henquin, J. C. (1998) Interplay between cytoplasmic Ca^{2+} and the ATP/ADP ratio: a feedback control mechanism in mouse pancreatic islets. Biochem. J. **333**, 269–274

48 Ainscow, E. K. and Rutter, G. A. (2002) Glucose-stimulated oscillations in free cytosolic ATP concentration imaged in single islet β cells: evidence for a Ca^{2+}-dependent mechanism. Diabetes **51**, S162–S170

49 Gruber, H. E., Hoffer, M. E., McAllister, D. R., Laikind, P. K., Lane, T. A., Schmid-Schoenbein, G. W. and Engler, R. L. (1989) Increased adenosine concentration in blood from ischemic myocardium by AICA riboside. Effects on flow, granulocytes, and injury. Circulation **80**, 1400–1411

50 Ainscow, E. K. and Rutter, G. A. (2001) Mitochondrial priming modifies Ca^{2+} oscillations and insulin secretion in pancreatic islets. Biochem. J. **353**, 175–180

51 Grapengiesser, E., Gylfe, E. and Hellman, B. (1989) Three types of cytoplasmic Ca^{2+} oscillations in stimulated pancreatic β-cells. Arch. Biochem. Biophys. **268**, 404–407

52 Theler, J.-M., Mollard, P., Guérineau, N., Vacher, P., Pralong, W.-F., Schlegel, W. and Wollheim, C. B. (1992) Video Imaging of cytosolic Ca^{2+} in pancreatic β-cells stimulated by glucose, carbachol, and ATP. J. Biol. Chem. **267**, 18110–18117

53 Grynkiewicz, G., Poenie, M. and Tsien, R. Y. (1985) A new generation of Ca^{2+} indicators with greatly improved fluorescence properties. J. Biol. Chem. **260**, 3440–3450

54 Varadi, A., Ainscow, E. K., Allan, V. J. and Rutter, G. A. (2002) Involvement of conventional kinesin in glucose-stimulated secretory-granule movements and exocytosis in clonal pancreatic β-cells. J. Cell. Sci. **115**, 4177–4189

55 Meisse, D., Van de Casteele, M., Beauloye, C., Hainault, I., Kefas, B., Rider, M., Foufelle, F. and Hue, L. (2002) Sustained activation of AMP-activated protein kinase induces c-Jun N-terminal kinase activation and apoptosis in liver cells. FEBS Lett. **526**, 38–42

56 Ido, Y., Carling, D. and Ruderman, N. (2002) Hyperglycemia-induced apoptosis in human umbilical vein endothelial cells: inhibition by the AMP-activated protein kinase activation. Diabetes **51**, 159–167

57 Blazquez, C., Geelen, M. J., Velasco, G. and Guzman, M. (2001) The AMP-activated protein kinase prevents ceramide synthesis de novo and apoptosis in astrocytes. FEBS Lett. **489**, 149–153

58 Wollheim, C. B., Kikuchi, M., Renold, A. E. and Sharp, G. W. (1977) Somatostatin- and epinephrine-induced modifications of $^{45}Ca^{2+}$ fluxes and insulin release in rat pancreatic islets maintained in tissue culture. J. Clin. Invest. **60**, 1165–1173

59 Wollheim, C. B., Winiger, B. P., Ullrich, S., Wuarin, F. and Schlegel, W. (1990) Somatostatin inhibition of hormone release: effects on cytosolic Ca^{2+} and interference with distal secretory events. Metab. Clin. Exp. **39**, 101–104

60 Habinowski, S. A., Hirshman, M., Sakamoto, K., Kemp, B. E., Gould, S. J., Goodyear, L. J. and Witters, L. A. (2001) Malonyl-CoA decarboxylase is not a substrate of AMP-activated protein kinase in rat fast-twitch skeletal muscle or an islet cell line. Arch. Biochem. Biophys. **396**, 71–79

61 Corkey, B. E., Deeney, J. T., Yaney, G. C., Tornheim, K. and Prentki, M. (2000) The role of long-chain fatty acyl-CoA esters in β-cell signal transduction. J. Nutr. **130**, 299S–304S

62 Liang, Y. and Matschinsky, F. M. (1991) Content of CoA-esters in perifused rat islets stimulated by glucose and other fuels. Diabetes **40**, 327–333

63 Bollheimer, L. C., Skelly, R. H., Chester, M. W., McGarry, J. D. and Rhodes, C. J. (1998) Chronic exposure to free fatty acid reduces pancreatic β cell insulin content by increasing basal insulin secretion that is not compensated for by a corresponding increase in proinsulin biosynthesis translation. J. Clin. Invest. **101**, 1094–1101

64 Iynedjian, P. B. (1993) Mammalian glucokinase and its gene. Biochem. J. **293**, 1–13

65 Sekine, N., Cirulli, V., Regazzi, R., Brown, L. J., Gine, E., Tamarit-Rodriguez, J., Girotti, M., Marie, S., MacDonald, M. J., Wollheim, C. B. and Rutter, G. A. (1994) Low lactate dehydrogenase and high mitochondrial glycerol phosphate dehydrogenase in pancreatic β-cell. Potential role in nutrient sensing. J. Biol. Chem. **269**, 4895–4902

66 Zhao, C., Wilson, C. M., Schuit, F., Halestrap, A. P. and Rutter, G. A. (2001) Expression and distribution of lactate/monocarboxylate transporter (MCT) isoforms in pancreatic islets and the exocrine pancreas. Diabetes **50**, 361–366

67 Randle, P. J., Garland, P. J., Hales, C. N. and Newsholme, E. A. (1963) The glucose fatty acid cycle: its role in insulin sensitivity and the metabolic disturbances of diabetes mellitus. Lancet **i**, 7285–7289

68 Liang, Y., Bai, G., Doliba, N., Buettger, C., Wang, L., Berner, D. K. and Matschinsky, F. M. (1996) Glucose metabolism and insulin release in mouse βHC9 cells, as model for wild-type pancreatic β-cells. Am. J. Physiol. Endocrinol. Metab. **270**, E846–E857

69 Zhao, C. and Rutter, G. A. (1998) Overexpression of lactate dehydrogenase A attenuates glucose-induced insulin secretion in stable MIN-6 β-cell lines. FEBS Lett. **430**, 213–216

70 Deeney, J. T., Gromada, J., Hoy, M., Olsen, H. L., Rhodes, C. J., Prentki, M., Berggren, P. O. and Corkey, B. E. (2000) Acute stimulation with long chain acyl-CoA enhances exocytosis in insulin secreting cells (HIT T-15 and NMRI β-cells). J. Biol. Chem. **275**, 9363–9368

71 Song, X. M., Fiedler, M., Galuska, D., Ryder, J. W., Fernstrom, M., Chibalin, A. V., Wallberg-Henriksson, H. and Zierath, J. R. (2002) 5-Aminoimidazole-4-carboxamide ribonucleoside treatment improves glucose homeostasis in insulin-resistant diabetic (ob/ob) mice. Diabetologia **45**, 56–65

72 Iglesias, M. A., Ye, J. M., Frangioudakis, G., Saha, A. K., Tomas, E., Ruderman, N. B., Cooney, G. J. and Kraegen, E. W. (2002) AICAR administration causes an apparent enhancement of muscle and liver insulin action in insulin-resistant high-fat-fed rats. Diabetes **51**, 2886–2894

73 Zhou, G., Myers, R., Li, Y., Chen, Y., Shen, X., Fenyk-Melody, J., Wu, M., Ventre, J., Doebber, T., Fujii, N. et al. (2001) Role of AMP-activated protein kinase in mechanism of metformin action. J. Clin. Invest. **108**, 1167–1174

Received 20 November 2002/10 February 2003; accepted 17 February 2003
Published as BJ Immediate Publication 17 February 2003, DOI 10.1042/BJ20021812

© 2003 Biochemical Society